Rock and Soil Mechanics 2025 46(2): 527−538 ISSN 1000−7598
https://doi.org/10.26599/RSM.2024.94300118 journal homepage: rocksoilmech.whrsm.ac.cn

Effect of initial consolidation inclination on strain development in saturated silty soil

FARHAD Jamil[1], ZENG Chang-nü[1], MA Yuan[2], SHARAFAT Ali[1]

1. School of Civil Engineering and Architecture, Henan University of Technology, Zhengzhou, Henan 450001, China

2. China Shanxi Sijian Group Co., Ltd., Taiyuan, Shanxi 030012, China

Abstract: This study investigates the strain development of saturated silty soil of Yellow River under varying initial consolidation inclination angles ζ by principle stress rotation tests. The results revealed that distinct patterns in axial, circumferential and torsional shear strains show the influence of ζ on the mechanical response of silty soil. Notably, the axial strain exhibits compressive behaviour at ζ=90° during the first cycle, while the circumferential strain displays tensile behaviour. Anisotropy initiates at ζ=90° and around 60° for other ζ angles. Different values of ζ exhibit stabilization trends in strain fluctuations, with ζ=90° and ζ=75° showing intriguing similarities. The case of ζ=45° stands out, with the highest fluctuation and strain amplitude. Torsional shear strain similarities are observed among most ζ angles except for ζ=90° and ζ=60° . Volumetric strain emphasizes the significant impact of consolidation angle inclination on anisotropic characteristics. With the increase of the initial solidification angle, the hysteresis curve shifts to the left, indicating cyclic creep characteristics, with negligible shear strain for the case of ζ=60° . As the cycle period increases, the hysteresis loop contracts, indicating the continuous strengthening and eventual stabilization of shear stiffness. This comprehensive exploration provides valuable insights into the complex behaviour of saturated silty soil under rotational stress conditions, highlighting the role of initial consolidation inclination angles in shaping its mechanical response.

Keywords: hollow cylindrical apparatus; principal stress rotation; inclined consolidation angle; silty soil; stress path

1 Introduction

The Yellow River is renowned for its elevated sediment load, resulting in the deposition of fine-grained substances along its downstream sections. The soils of the lower Yellow River Zone are predominantly silty in nature primarily consisting of minute particles, with a significant proportion being silt. Silty soils frequently exhibit a propensity for consolidation and settlement under loads, thereby impacting their shear strength and presenting notable difficulties in the realm of construction endeavours[1]. Silty sand mixtures with a substantial silt content exhibit a greater inclination to flow in comparison to pure sand. Moreover, the response of silty sands is also influenced by the quantity of fines within the sand. Examining the deformation characteristics of silty soil subjected to inclined consolidation angles constitutes a pivotal aspect in the realm of geotechnical engineering. This aspect exerts a direct influence on the stability and subsidence of structures erected on or in proximity to silty soils. Due to the aforementioned challenges, it is necessary to investigate the mechanical behaviour of Yellow River silty soil under the drainage condition by considering the principal stress rotation angle and initial consolidation angle. Performing a comprehensive investigation is crucial in order to provide reliable recommendations for infrastructure projects. In this particular study, we extensively investigate the deformation characteristics of soil with a high silt content and its anisotropic properties. To be more precise, the research aims to examine the development of strain patterns.

The impact of the initial consolidation angle on the strain behaviour in silty soil is to enhance the soil's vulnerability to instability, while diminishing the shear strength subsequent to reaching its maximum value. Zhuang et al.[2] conducted triaxial experiments on silty soil, and their observations revealed that if the cyclic yield strain limits were not surpassed, the strength remained unchanged following consolidation. Nevertheless, they also discovered that surpassing a pore pressure ratio of 0 could lead to a notable decrease in volume and an augmentation in undrained shear strength. The aforementioned observation implies that the response of silty soil to inclined consolidation angles is affected by the magnitude of cyclic pre-loading and consolidation[3]. The behaviour of silty soil under inclined consolidation angles is an intricate and diverse phenomenon, influenced by numerous factors. Gaining insight into the response of silty soil under inclined consolidation angles is of utmost importance in order to accurately forecast soil behaviour and assess deformations.

In the context of varying consolidation angles, the rotation of the major principal stress is observed,

Received: 1 April 2024 Accepted: 22 August 2024
This work was supported by the Henan Province Joint Fund Project of Science and Technology (222103810075) and the Innovative Funds Plan of Henan University of Technology (2022ZKCJ07).
First author: FARHAD Jamil, male, born in 1989, PhD candidate, focusing on soil dynamics, soil rehabilitation. E-mail: jaaamfarhad@gmail.com
Corresponding author: ZENG Chang-nü, Female, born in 1978, PhD, Professor, mainly engaged in research on soil dynamics and engineering seismic resistance. E-mail: zengcnv@126.com

leading to a direct impact on the soil permeability and strength[4]. The orientation of the primary stress axis during the process of consolidation has the potential to impact the maximum shear resistance of the soil, leading to an enhanced resistance in both unconsolidated and modified soil samples[5]. Moreover, the evolution of strains and the hydraulic pressure within silty soil is affected by the magnitude of shear stress, as well as the angle of rotation of the primary stresses[6].

Until now, the majority of academics have examined the static and dynamic characteristics of soil based on isotropic or K_0 (consolidation with lateral constraints) anisotropic consolidation of soil[7−10]. In specific engineering situations, particularly those involving slope, subgrade and extensive excavation of foundation pits, it is feasible for the primary stress axis of soil to be inclined at different angles rather than being perpendicular to the horizontal direction during the consolidation process[11]. In the domain of constructing embankments in multiple stages, it is of utmost importance to take into account the consolidation of soil constituents. More precisely, soil components positioned at different locations beneath the central axis of the embankment will exhibit separate alignments of the primary stress intensity during the phenomenon known as inclined consolidation as illustrated in Fig. 1. Thus, consolidation that exhibits a tendency towards a particular direction can be categorized as a unique manifestation of anisotropic consolidation, wherein the principal stress orientation deviates from the vertical axis during the process of consolidation. This deviation is anticipated to have a significant influence on the soil's strength and strain development[12−15]. It is crucial to emphasize that this distinct form of anisotropy differs from previous studies and requires comprehensive investigation.

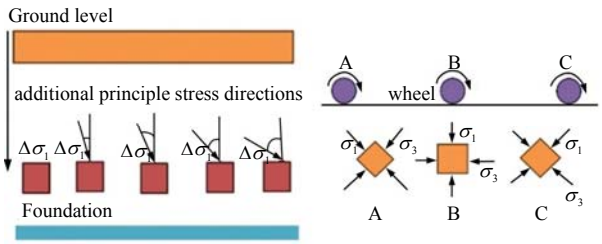

Fig. 1 Stress condition of soil under an embankment and traffic

2 Literature review

Currently, the extent of research concerning the phenomenon of inclined consolidation is currently limited in its scope. Nevertheless, the examination of stress modifications that transpire during the consolidation of subterranean constituents beneath multistage embankments through numerical simulation stands as a noteworthy contribution to this particular area of investigation[16]. A thorough examination was carried out to investigate the influence of anisotropy induced by inclined consolidation on the deformation and stiffness characteristics of densely packed silt specimens. The results of their study unveiled that inclined consolidation possesses the capability to alter the orientation of stiffness and yielding anisotropy axes to align with the initial consolidation angle[17]. A study[18] was carried out to investigate the relationship between the static undrained response of loosely packed sands and the level of the initial anisotropic stress condition. This was achieved by manipulating the primary principle stress orientation and other variables.

The triaxial test has gained significant popularity in the process of quantifying the mechanical properties of soils. However, a notable limitation of the conventional triaxial test lies in its ability to impose solely either a compressive or an extensive stress field on a soil element. However, in order to obtain a comprehensive and inclusive understanding of the behavior of soil under complex stress condition, it is of utmost importance to possess knowledge and comprehension of its reaction. The hollow cylindrical apparatus (HCA) has the capability to facilitate intricate stress paths that involve modifications to the primary directions of stress[18-21]. Numerous and persistent inquiries have been conducted to examine the behavior of silt, sand and clay using HCA particularly when subjected to stress paths involving modifications in the primary direction of principal stress identified as α and the coefficient of intermediate principal stress denoted as b[18, 22-26]. The variable represented by the symbol α signifies the degree of the angle, which represents the relationship between the primary stress direction and the vertical axis. This angle is denoted as $\alpha = \arctan\left(\dfrac{2\tau_{z\theta}}{\sigma_z - \sigma_\theta}\right)$, where $\tau_{z\theta}$ is the shear stress acting on the $z\theta$ plane, σ_z represents the normal stress acting in the z-axis direction, and σ_θ represents the normal stress acting in the circumferential or tangential direction. The intermediate principal stress coefficient is defined as $b = \dfrac{\sigma_2 - \sigma_3}{\sigma_1 - \sigma_3}$, where σ_1, σ_2, and σ_3 represent the maximum principal stress, the intermediate principal stress, and the minimum principal stress, respectively.

To this day, there have been a limited number of studies that have been undertaken in order to investigate the effects of the rotation of principal stress and the angle of consolidation on soil composed of silt particles[27−28]. HCA is utilized to conduct trials on fully saturated silt. These trials encompassed diverse ratios of cyclic loading amplitudes in both axial and torsional modes, as well as simulated circular and elliptical dynamic stress paths. These investigations unveiled the

significant influence of dynamic stress paths on the process of liquefaction in fully saturated silt.

The extensive occurrence of fine particles in the lower sections of the Yellow River region necessitates a thorough examination of its mechanical behavior under stress and strain for the purposes of economic development and infrastructure safety. The main objective of this investigation is to explore the effects of the rotation of principal stresses and the consolidation angles on the behavior of the silty soil using a cylindrical apparatus with a hollow core. Our research delves into the influence of the number of loading cycles on the static properties of fully saturated silty soil with a specific focus on the coefficient of principal stress (b) and the initial consolidation angle (ζ).

Our primary objective is to investigate the anisotropic properties of fully saturated silty soil under conditions of drainage. This exploration will encompass several dimensions, including stress relationships, deformation, changes in volume and strength. The valuable knowledge obtained from these experiments will contribute to a deeper comprehension of the stress state of subgrade soil in real-world engineering scenarios. Consequently, it will offer more accurate recommendations for road design and the development of infrastructure.

3 Research methodology

3.1 Test equipment

The present investigation utilizes HCA, a device that was developed by the UK-based GDS Company. This apparatus is employed to recreate complex stress conditions and imitate the stress state of the soil as it is observed in practical road engineering situations. The HCA is comprised of two primary components: the DYNTTS, which is the dynamic triaxial test system, and the DYNHCA, which is the dynamic hollow cylinder torsional shear test system. This system encompasses an axial/torsional driving device, a pressure chamber, controllers for internal and external confining and back pressure, a system for measuring stress and strain, a signal conditioning system and a GDS digital control system (DCS). The instrument for hollow cylindrical torsion shear can be observed in Figs. 2 and 3.

The torsion shear apparatus in the form of a hollow cylinder employs a sample with a hollow cylindrical shape. The height of this sample is denoted by H, with an additional measurement of 200 mm. It has an outer diameter r_o of 50 mm and an inner diameter r_i of 30 mm. In order to induce stress-strain components within the sample, the apparatus applies various external and internal pressures, namely the internal confining pressure P_i, the external pressure P_0, the axial force W and the torque T. The DYNHCA possesses the capacity to



Fig. 2 GDS hollow cylindrical apparatus

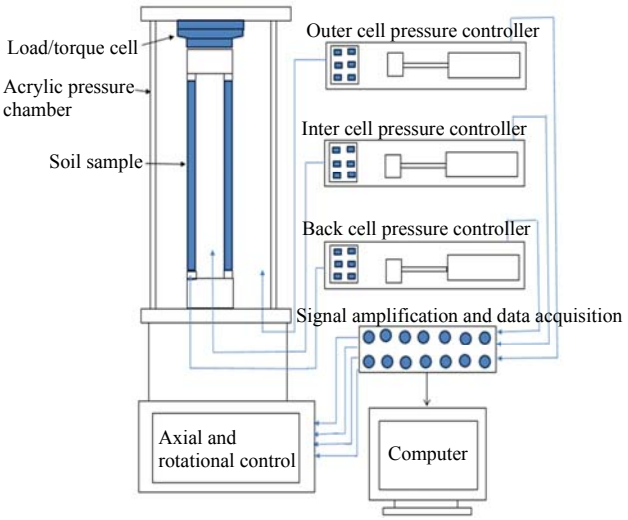

Fig. 3 Schematic diagram of HCA

generate the four stress elements, including the axial stress σ_z, the radial stress σ_r, the circumferential stress σ_θ and the torsional shear stress $\tau_{z\theta}$. Additionally, the four corresponding strain components can be produced and quantified. Through the combination of these stress and strain elements, the hollow cylindrical torsion shear apparatus can achieve intricate and continuous rotating stress paths. Fig. 4 presents the stress-strain state of the hollow cylindrical specimen throughout the testing procedure. The calculation formulas for the stress strain components is mentioned below.

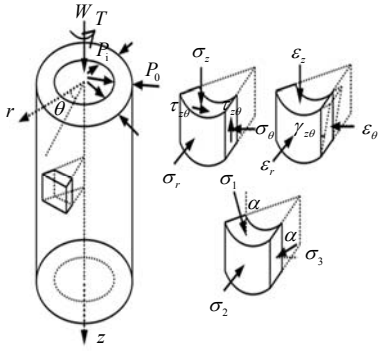

Fig. 4 Stress state of hollow cylindrical specimen

Table 1 Formulas used for stress strain components[18]

Component	Stress	Strain
Axial	$\sigma_z=\frac{W}{\pi(r_o^2-r_i^2)}+\frac{P_o r_o^2-P_i r_i^2}{r_o^2-r_i^2}$	$\varepsilon_z=\frac{z}{H}$
Radial	$\sigma_r=\frac{P_o r_o+P_i r_i}{r_o+r_i}$	$\varepsilon_r=-\frac{u_o-u_i}{r_o-r_i}$
Circumferential	$\sigma_\theta=\frac{P_o r_o-P_i r_i}{r_o-r_i}$	$\varepsilon_\theta=-\frac{u_o+u_i}{r_o+r_i}$
Shear	$\tau_{z\theta}=\frac{3T}{2\pi(r_o^3-r_i^3)}$	$\gamma_{z\theta}=\frac{2\theta(r_o^3-r_i^3)}{3H(r_o^2-r_i^2)}$
Major Principal	$\sigma_1=\frac{\sigma_z+\sigma_\theta}{2}+\sqrt{\left(\frac{\sigma_z-\sigma_\theta}{2}\right)^2+\tau_{z\theta}^2}$	$\varepsilon_1=\frac{\varepsilon_z+\varepsilon_\theta}{2}+\sqrt{\left(\frac{\varepsilon_z-\varepsilon_\theta}{2}\right)^2+\gamma_{z\theta}^2}$
Intermediate Principal	$\sigma_2=\sigma_r$	$\varepsilon_2=\varepsilon_r$
Minor Principal	$\sigma_3=\frac{\sigma_z+\sigma_\theta}{2}-\sqrt{\left(\frac{\sigma_z-\sigma_\theta}{2}\right)^2+\tau_{z\theta}^2}$	$\varepsilon_3=\frac{\varepsilon_z+\varepsilon_\theta}{2}-\sqrt{\left(\frac{\varepsilon_z-\varepsilon_\theta}{2}\right)^2+\gamma_{z\theta}^2}$

Note: z is the axial displacement of the sample, with compression being positive and tension being negative; u_o and u_i represent the displacements of the outer diameter and inner diameter of the sample, respectively; θ represents the rotational displacement of the sample, with clockwise rotation being negative and counterclockwise rotation being positive.

3.2 Test plan

The silty soil in this article serves as the experimental material from the track foundation of Zhengzhou Metro Line 1. The physical properties of the samples used in this paper are as follows: specific gravity G_s of 2.63, moisture water content of 23.54%, density ρ of 1.64 g/cm^3, maximum void ratio e_{max} of 0.93, minimum void ratio e_{min} of 0.51, coefficient of uniformity C_u of 4.43, curvature coefficient C_c of 1.19, liquid limit is 28.6%, plastic limit is 19.6%, and plasticity index is 8.7. The provided data on particle grading curve can be observed in Fig. 5.

At present, there are various methods for preparing hollow cylindrical specimens. For sandy soil, there are sand drop method, water vibration method and wet compaction method. For clay, sometimes thin-walled pipe cutting method is used to obtain undisturbed clay. The material selected in this article is silty soil, so the sand drop method is used to fill the sample layer by layer during the sample preparation process. The sand drop method allows for a more realistic simulation of the in-situ conditions of silty soils, particularly in terms of density and structure, similar to previous study[29]. The sample components are prepared by cleaning and wiping them with water, and the molds and pipelines are inspected in the pressure chamber to prevent pipeline blockage caused by silt. The outer rubber mold is used to ensure leak-free using visual, air blowing, or water filling inspections. The inner membrane with a metal snap ring and O-ring is assembled for sealing, while the petroleum gel is applied to the base card slot to prevent damage. Petroleum gel is known for its lubricating properties. When the petroleum gel is added, it can reduce friction between soil particles, making it non-sticky with the side walls[30]. The permeable stone is inserted and tighten. The filter paper is placed on the permeable stone and covers the outer membrane on the base outer wall. The outer three petal mold is secured with rubber bands or fixtures. A sample space of 200 mm×50 mm×30 mm was selected to minimize stress non-uniformities and ensure that a central high area is not affected by boundary conditions[31]. They also suggested that a satisfactory geometry of the hollow cylinder specimen with regard to non-uniformity and experimental control would be obtained if r_i/r_o is within 0.65 to 0.82[31]. The present study has r_i/r_o=0.8. To reduce the influence of radial friction, the height was recommended as $H/2r_o$=1.8–2.2. The present study employs $H/2r_o$= 200/100 mm = 2.

The test plan for the series of pure rotation of the principal stress axis is presented in Table 2. In this study, the coefficient of the intermediate principal stress is kept constant. Although this is a limitation of the study, the constant coefficient ensures that the intermediate principal stress is consistently applied in all tests, resulting in more comparable and reproducible results, as reported in the previous research[32]. During the setup stage, an initial effective stress of 40 kPa was applied using a vacuum. Subsequently, pore pressure and cell pressure were simultaneously increased. The specimen was then saturated, ensuring that the B-value (the ratio of pore water pressure to confining pressure[33]) reached 0.97 or higher. After achieving this

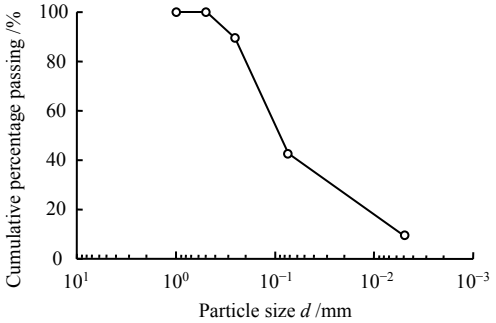

Fig. 5 Particle grading curve of silty soil

Table 2 Pure stress rotation test scheme

Serial Number	Initial consolidation inclination angle ζ /(°)	Coefficient intermediate principal stress b	Deviatoric stress q /kPa	Effective mean principal stress p'/kPa	Rotation range α /(°)	Shear rate /((°)/min)
D101	15					
D102	30				Angle after	
D103	45	0.5	140	150	Consolidation–1 800	8
D104	60					
D105	75					
D106	90					

saturation, the specimen was isotropically consolidated in multiple stages, resulting in an effective mean stress of 150 kPa. In this study, the angle α was increased up to 360° to emphasize the first two cycles (each cycle with a rotation of 180° of the principal stresses), as the soil's response to pure principal stress rotation is most significant during the initial cycles, as documented in references[25, 26, 34]. Twelve tests were conducted for D series. Subsequently, the consolidation b and the shear stress q were gradually increased to the values listed in Table 2 under undrained conditions, maintaining a constant p'=150 kPa until the shearing stage. Based on the experimental configuration, the correlation between the stress path in the experiment and the rotation angle of the principal stress axis can be observed in Fig. 6.

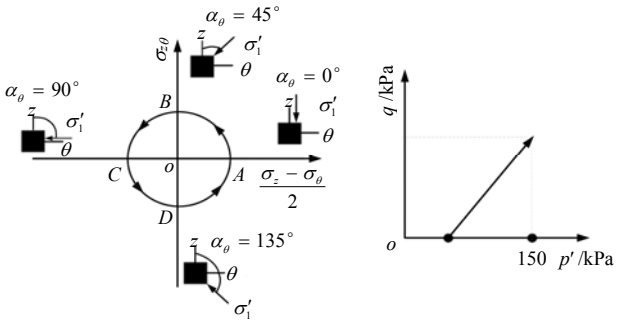

Fig. 6 Stress path of pure principal stress rotation test

Due to the compression of water pressure during the saturation and consolidation process of the sample, r_o and r_i will undergo changes, as the acquisition of r_o and r_i is calculated based on the changes in internal and external confining pressure, back pressure and vertical displacement. After the change, the calculation formulas for r'_o and r'_i are as follows:

$$r'_o = \sqrt{\frac{r_o^2 H}{H'} - \frac{\Delta V_S + \Delta V_i}{\pi H'}} = \sqrt{\frac{r_o^2 H}{H - \Delta H} - \frac{\Delta V_S + \Delta V_i}{\pi (H - \Delta H)}} \quad (1)$$

$$r'_i = \sqrt{\frac{r_i^2 H}{H'} - \frac{\Delta V_i}{\pi H'}} = \sqrt{\frac{r_i^2 H}{H - \Delta H} - \frac{\Delta V_i}{\pi (H - \Delta H)}} \quad (2)$$

where ΔV_S represents the volume change of the sample, the drainage is positive; ΔV_i is the volume change in the inner cavity of the sample, and the drainage is positive; and H' is the height of the sample after consolidation.

Figure 7(a) illustrates the variation of internal and external confining pressures during the shear process. P'_i and P'_o represent the inner confining pressure and the outer confining pressure, respectively. Fig. 7(b) shows the variation of axial force and torque during the shear process, with axial force ranging from −0.6 kN to 0.6 kN and torque ranging from −15 kN • m to 15 kN • m. Repeatability of test can be followed similar to the previous study[35].

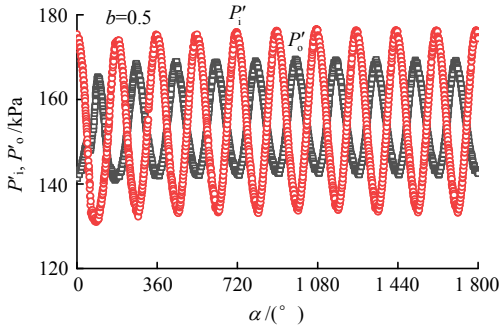

(a) Variation of P'_i and P'_o during the shear processs

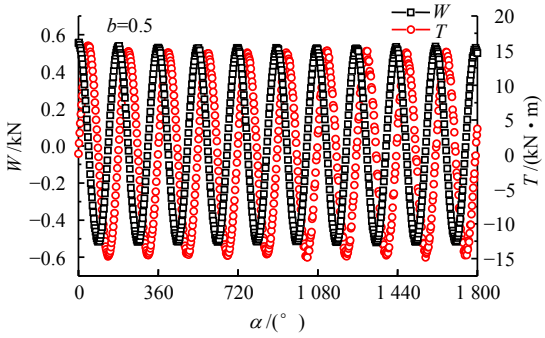

(b) Variation of W and T during the shear process

Fig. 7 Changes in internal and external confining pressures, axial force and torque during shearing process

4 Results and discussion

4.1 Strain development pattern under different consolidation angles

We examined the deformation response caused by the rotation of primary stresses at different initial consolidation angles (ζ) with $b = 0.5$. Figs. 8 to 12 illustrate the strain development pattern of silty soil. These figures represent the distinct variations in deformation observed in silty soil across different directions, which are linked to the specific initial consolidation angles employed.

4.1.1 Axial strain

Figure 8 presents the evolution of axial strain under different initial consolidation angles ζ. During the initial rotation period (0° to 180°), the distinction between ζ=90° and other angles is well-noted. At ζ=90°, there is a compressive strain that increases and then decreases, while other angles exhibit tensile strain following a similar increasing and then decreasing pattern. The maximum axial compressive strain at ζ=90° is approximately 4.2% and maximum axial tensile strain at ζ=15° and ζ=30° is almost −4.7% (where the negative sign shows the tension). This indicates a fundamental difference in the response of soil to initial consolidation angles. As the principal stress axis continues rotating in the third cycle (360° to 540°), the fluctuation amplitude of axial strain in silty soil tends to stabilize for all considered angles ζ, indicating that the soil undergoes a stress relaxation

process in response to constantly changing stress conditions. Upon examining the figure, it becomes evident that at ζ = 0°, axial strain is nearly zero, displaying minimal amplitude changes. As ζ increases beyond 0°, it generates axial compressive strain, with larger ζ values, resulting in greater compressive strain. Conversely, when ζ is less than 0°, axial tensile strain occurs and smaller ζ values lead to more significant tensile strain. This variation in strain behavior provides valuable insights into the intricate relationship between consolidation inclination and axial strain. At ζ = 90°, anisotropy becomes apparent as the principal stress axis initiates rotation, emphasizing the perpendicular orientation of the consolidation inclination angle and its profound influence on the silty soil deformation characteristics. For other ζ angles, anisotropy becomes noticeable at approximately 60° of sample rotation, highlighting the role of consolidation inclination in shaping the strain response during stress axis rotation. The findings align with existing studies that emphasize the impact of consolidation conditions on soil deformation characteristics. The observed trends in axial strain behavior can be linked to the fundamental principles of soil mechanics, where initial consolidation conditions influence the anisotropic nature of soil response under cyclic loading[15, 35].

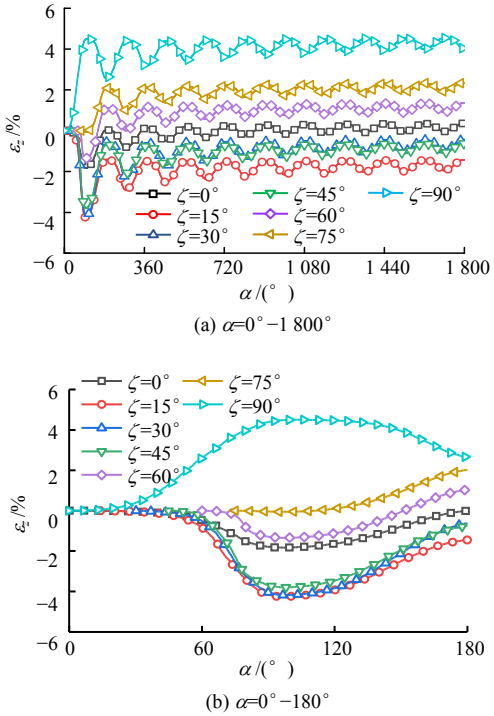

Fig. 8 Axial strain development pattern under different consolidation angles ζ

4.1.2 Circumferential strain

Figure 9 illustrates the development pattern of circumferential strain under varying ζ angles during the rotation period. In the first rotation cycle (0° to 180°), when ζ=90°, circumferential tensile strain initially increases and then decreases, whereas for all other ζ values, there is an initial increase followed by a decrease in axial compressive strain. As the stress axis continues its rotation, it's evident that the circumferential strain curves for ζ angles of 0°, 30°, 75° and 90° have reached a stable state. In contrast, for ζ angles of 15°, 60° and 45°, the circumferential strain values are still on the rise. In the tenth rotation cycle, the circumferential strain at ζ=90° is negative, fluctuates around 0 at ζ=75°, and remains positive for the remaining ζ angles.

Notably, the most pronounced anisotropic characteristic is observed at ζ=45°, with the highest amplitude of circumferential strain fluctuation and the largest circumferential strain value, indicating that the consolidation angle has a significant influence on deformation behavior. This specific angle results in distinctive strain patterns. A different behavior is noticed when the rotation reaches ζ=30°, where the specimens also exhibit anisotropic characteristics. This distinct behavior suggests that, at ζ=30°, the specimens exhibit anisotropic characteristics, contributing to the overall complexity of strain development.

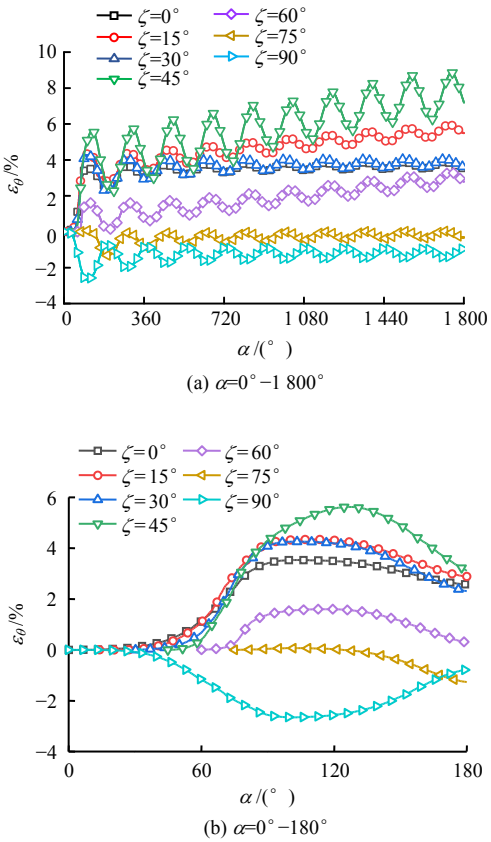

Fig. 9 Circumferential strain development pattern under different ζ

4.1.3 Radial strain

From Fig. 10, we can observe the distinct development patterns of radial strain under varying ζ angles during the rotation period, especially in the first cycle. In this

initial cycle, noticeable anisotropy is already evident among the samples. This early anisotropic behaviour suggests that the consolidation inclination angle ζ plays a significant role in shaping radial strain responses during stress axis rotation. The development pattern curve differs notably between ζ=15° and ζ=30°, underscoring the sensitivity of radial strain to subtle changes in consolidation inclination angles. This sensitivity contributes to the overall complexity of silty soil deformation. Particularly, the case of ζ=45° displays substantial anisotropy from the initiation of stress axis rotation, maintaining the highest radial strain amplitude and radial strain value throughout the entire rotation cycle. Similar to circumferential strain, it rotates continuously with the main stress axis. The circumferential strain curves at ζ 0°, 30°, 75°, and 90° are stabilized, indicating a settling or equilibrium state in response to stress axis rotation. This stability is observed in circumferential strain, emphasizing the influence of ζ on overall soil sample deformation, as the circumferential strain values of ζ 15°, 60° and 45° are still increasing. Interestingly, the development curves of radial strain at ζ=75° and ζ=90° closely coincide during the continuous rotation of the primary stress axis with little observable anisotropy in this particular case. The soil exhibits similar mechanical behavior at these angles due to the stress axis' near-vertical orientation relative to the consolidation direction. The closeness in strain response suggests that the soil's fabric and structure are not greatly altered between these two orientations, resulting in identical deformation patterns[36−37].

4.1.4 Torsional shear strain

Figure 11 reveals that, aside from ζ=90° and ζ=60°, the development pattern of torsional shear strain under various ζ angles is quite similar. This commonality emphasizes the influence of ζ on torsional shear behavior. In the first cycle, the cases of ζ=90° and ζ=75° display a pattern of torsional shear tensile strain that initially increases and then decreases. This behavior indicates a dynamic response to stress axis rotation, with a fluctuation in torsional shear strain amplitude, similar to the previous study[38]. For ζ ranging from 0° to 60°, torsional shear tensile strain follows the same increasing and decreasing trend, with the highest fluctuation amplitude of 0.006% occurring at ζ=60°. Eventually, it stabilizes at around 0.002%, nearly 0%, and the consistent trend across these angles

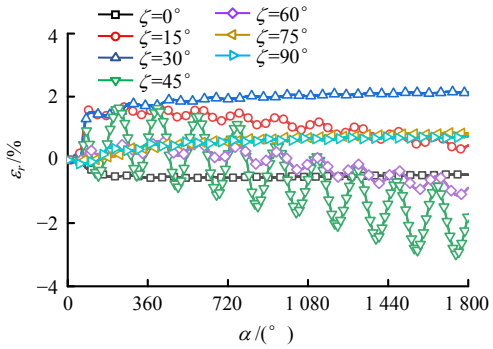

(a) α=0°−1 800°

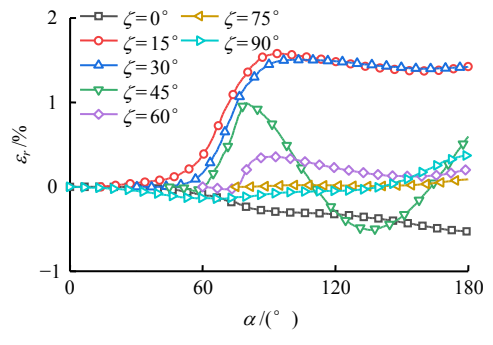

(b) α=0°−180°

Fig. 10 Radial strain development under different ζ

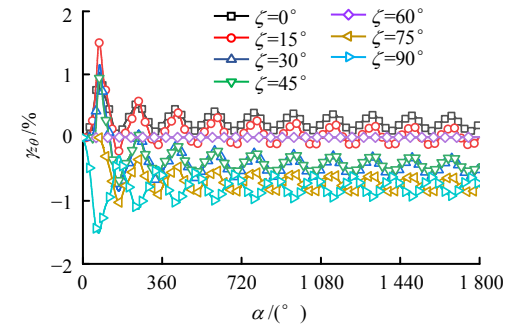

(a) α=0°−1 800°

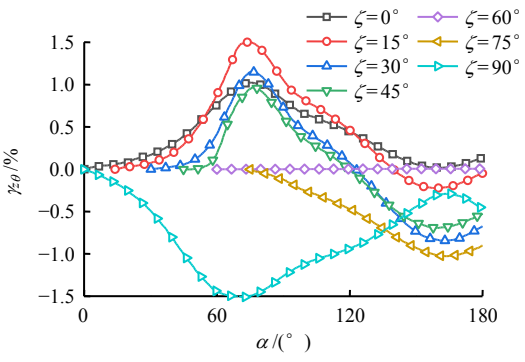

(b) α=0°−180°

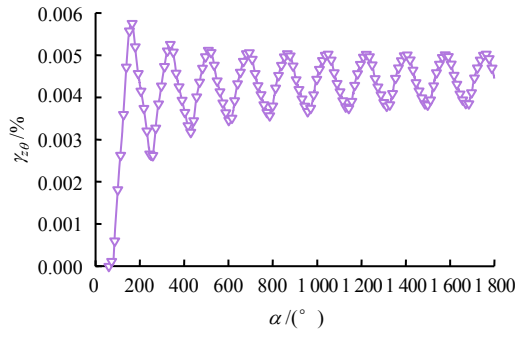

(c) Amplified view at ζ=60°

Fig. 11 Torsional shear strain development under different ζ

suggests a shared sensitivity to stress axis rotation. Interestingly, the development curve for ζ=30° and ζ=45° of torsional shear strain closely coincides during the continuous rotation of the principal stress axis, showing little observable anisotropy. This alignment in the behavior suggests that these angles share similar torsional shear responses to stress axis rotation.

4.1.5 Volumetric strain

To investigate variations in the strain development of saturated silty soil under different ζ values, one can refer to Fig. 12. In this figure, if volumetric strain (ε_v) is greater than 0, it indicates that the sample is in a drained state, resulting in sample volume decrease or shrinkage. The pattern of volumetric strain change under the influence of different values is largely consistent across various ζ angles. The rate of volumetric strain exhibits a linear increase in the initial two cycles (0°−360°), suggesting a common response of the saturated silty soil to stress axis rotation during this phase. However, beyond 360°, the growth rate of volumetric strain at ζ=0°, 60°, 75° and 90° gradually slows down. This behaviour indicates a diminishing rate of volume change, suggesting a stabilization or reduction in the shrinkage process. Meanwhile, at ζ=15°, 30° and 45°, the rate of volumetric strain continues to rise rapidly beyond 360°, implying that under these ζ angles, the silty soil continues to undergo significant volumetric changes, possibly due to ongoing consolidation. Notably, the sample at ζ=75° experiences the least shrinkage, while the sample at ζ=30° undergoes the most significant shrinkage. This suggests that the consolidation angle (ζ) has a substantial impact on the volumetric behaviour of the saturated silty soil, with different angles leading to varying degrees of shrinkage. In comparison with the volumetric strain under different principal stresses discussed earlier, the impact of consolidation angle on volumetric strain is more pronounced, leading to clearer anisotropic characteristics.

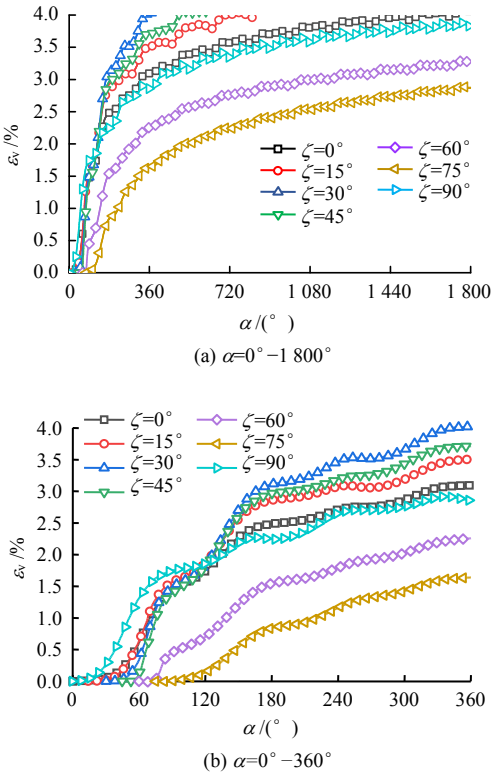

Fig. 12 Volumetric strain development pattern under different ζ

4.2 Shear stress and strain development under different inclination consolidation angles

Figure 13 depicts the shear stress and shear strain development curves of test series under various cycle numbers in principle stress rotation test with a fixed initial consolidation inclination angle. To facilitate observation, representative curves from different ζ values, specifically those from the 1st, 2nd, 3rd, 5th, 7th, and 10th cycles, were chosen for analysis.

Observing Fig. 13(a) to 13(g), it is evident that, irrespective of the initial consolidation inclination angle, the shear stress-shear strain relationship curves exhibit distinct hysteresis characteristics. For ζ=15°, ζ=30°, and ζ=45°, the shapes of the shear stress and shear strain hysteresis loops are similar, while ζ=75° and ζ=90° also share similar loop shapes, indicating a consistent response in terms of hysteresis loop characteristics for these specific ζ angles. As the cycle period increases, the hysteresis loop transitions from an unclosed to a closed state, indicating the changes in the silty soil response to stress over successive cycles. As each cycle's hysteresis loop contracts, the shear strain amplitude decreases with cycle period, signifying the continuous strengthening and eventual stabilization of shear stiffness. Notably, with an increase in the initial consolidation inclination angle, the hysteresis curve shifts leftward, indicating cyclic creep characteristics[39]. The case of ζ=60° serves as the boundary for creep in the hysteresis curve, where shear strain becomes extremely small, as illustrated in Fig. 13(d). This leftward shift suggests a greater tendency for cyclic creep at higher consolidation angles.

Figure 14 illustrates the evolution of shear strain at various ζ angles during the 1st, 3rd, and 10th cycles of the pure principle stress rotation test. The figure also highlights that with the increase in the initial consolidation inclination angle, the hysteresis curve consistently shifts leftward, indicating that higher consolidation angles will result in a greater tendency for cyclic creep and reduced shear strain. Simultaneously, as the cycle period extends, the sample tends towards stability, which implies that over consecutive cycles, the soil undergoes changes in its shear strain behaviour, eventually reaching a more stable state, and the hysteresis curve after stabilization at different initial consolidation inclination angles nearly aligns with the shear strain angle on the coordinate's horizontal axis.

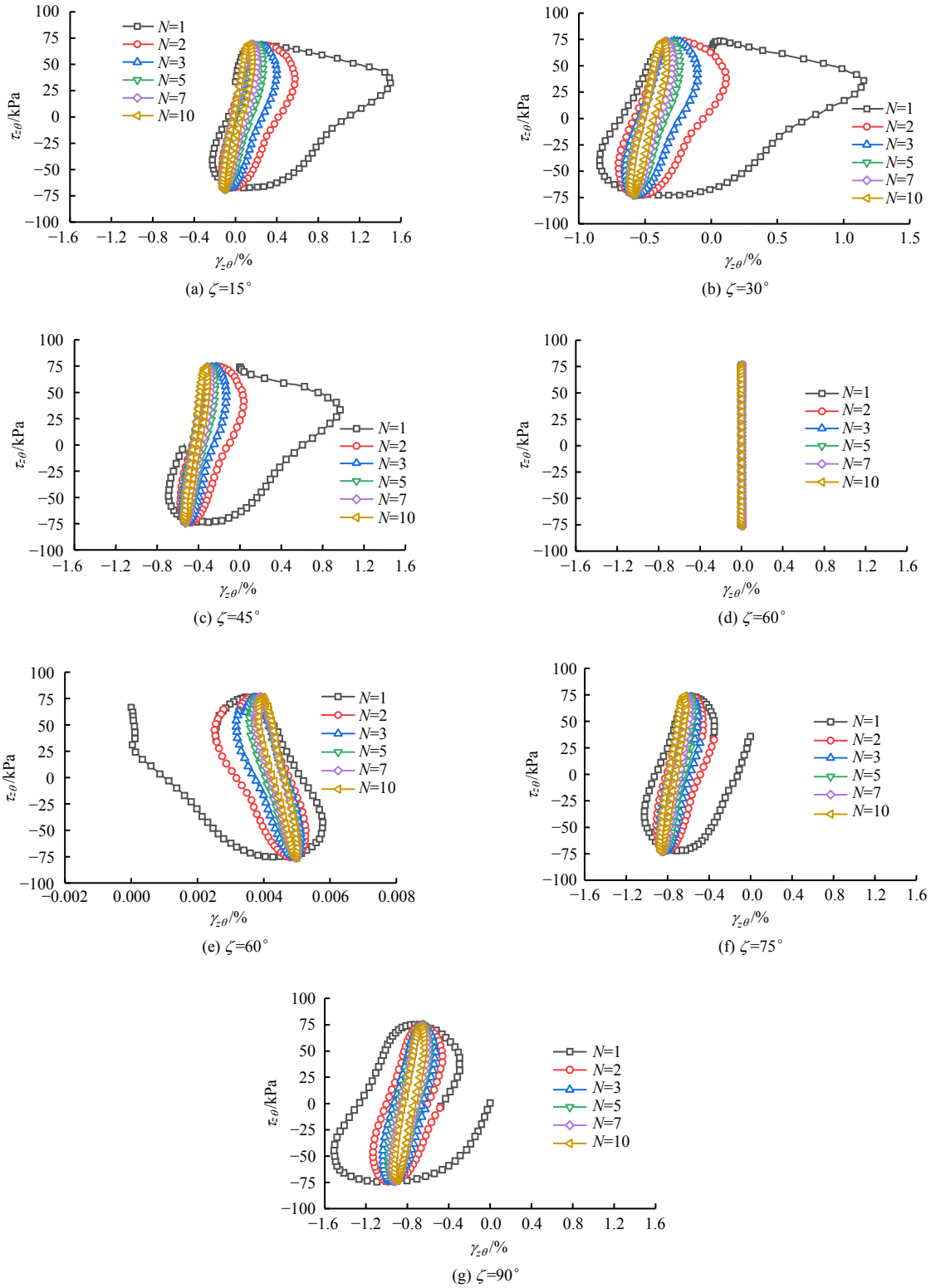

Fig. 13 Shear strain development pattern under different number of cycles with fixed ζ

Notably, the curves from the two sets of consolidation inclination tests, i.e, ζ=30° and ζ=45°, as well as ζ=75° and ζ=90°, there is significant overlap during the first cycle. This indicates a minimal difference in shear stress and strain anisotropy between these two groups, and the overlap in curves implies that these specific consolidation angles have similar shear strain responses during the initial cycle.

4.3 Non-coaxial behavior of silty soil

Many laboratory test findings suggest that geo-materials consistently exhibit non-coaxiality. Non-coaxiality is characterized as the absence of alignment between the principal stress direction and the principal strain increment direction. Several scholars have directed their attention towards the non-coaxial behavior of soil and have discovered that it significantly impacts the

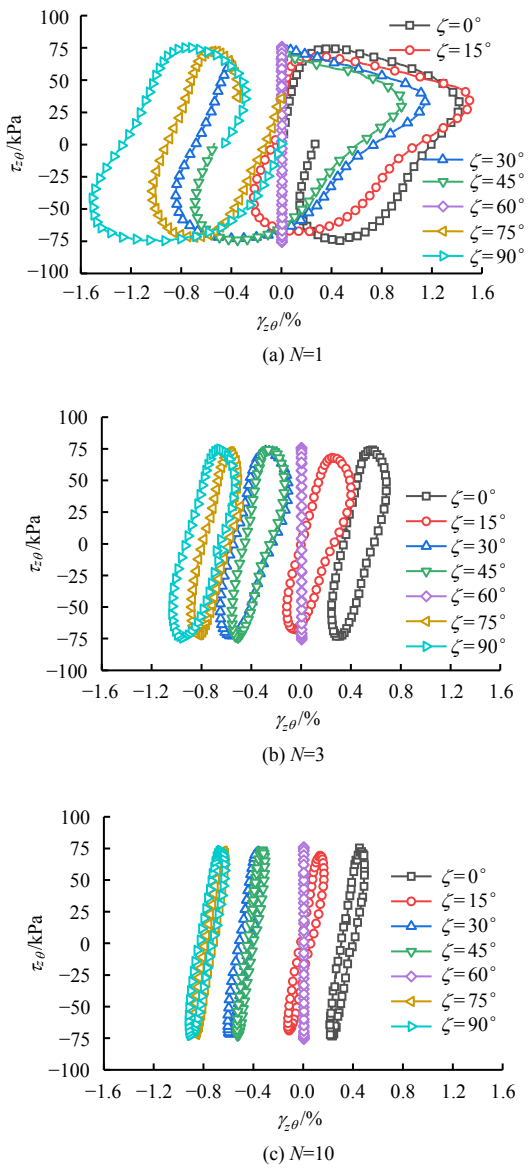

(a) N=1

(b) N=3

(c) N=10

Fig. 14 Shear strain development pattern at different ζ

analysis and design in geotechnical engineering. Neglecting the influences of non-coaxiality in geotechnical design may lead to potential hazards[40-43]. It is difficult to differentiate between the elastic strain increment and the total strain increment. Gutierrez et al.[40] conducted studies which suggest that the elastic strain increment can be ignored due to its significantly smaller contribution to the total strain increment compared to the plastic strain increment. Instead of focusing on the plastic strain increment, the analysis of non-coaxiality utilizes the total strain increment. The non-coaxiality is denoted by β and can be defined as the angle between the principal stress directions α and the direction of the principal strain increment $\beta \mathrm{d}\varepsilon$.

$$\beta = \beta \mathrm{d}\varepsilon - \alpha \tag{3}$$

$$\beta \mathrm{d}\varepsilon = \frac{1}{2}\tan^{-1}\frac{\mathrm{d}\gamma_{z\theta}}{\mathrm{d}\varepsilon_z - \mathrm{d}\varepsilon_\theta} \tag{4}$$

To examine how the initial major principal stress direction (α) impacts non-coaxiality, Fig. 15 illustrates the relationship between non-coaxiality degrees during the first rotation period (N1: 0°–180°) and the third rotation period (N3: 360°–540°). Various initial major principal stress directions (ζ = 15°, 30°, 45°, 60°, 75° 90°) under b= 0.5 are plotted against the major principal stress direction. While some similar patterns emerge, distinct evolutions occur for different initial major principal stress directions. Notably, the initial degree of non-coaxiality is roughly 45° at the beginning of loading. The variation of non-coaxiality is identical when ζ = 15° and ζ = 90°, contrasting with ζ=45°. Similarly, the non-coaxiality variation is the same for ζ = 30° and ζ = 60°. The major principal stress direction corresponding to the peak ζ-angle value varies; for instance, there is a difference of 15° between the peak values of ζ = 15° and ζ = 90°. This indicates that the non-coaxiality of soft clay is influenced by the initial major principal stress direction. However, the maximum and minimum values of non-coaxiality in each period are approximately the same, suggesting that the impact of α on these extreme values is minimal.

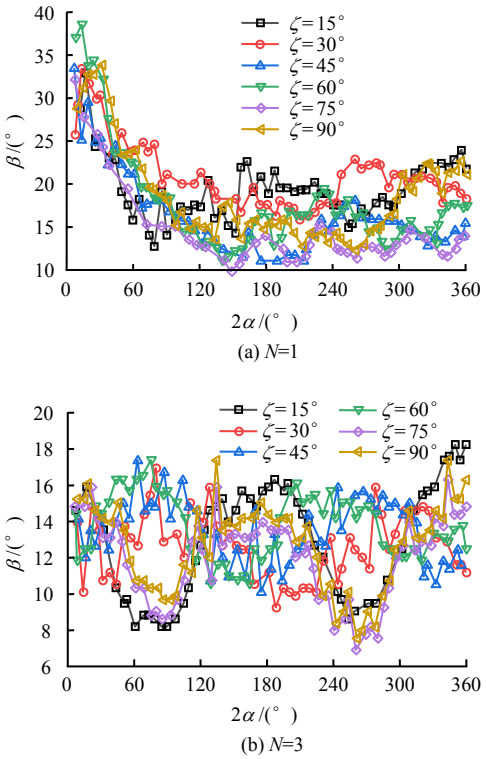

(a) N=1

(b) N=3

Fig. 15 The relationship between degrees of non-coaxiality and principal stress direction with b = 0.5

5 Conclusion

The main findings can be summarized as follows:

（1） At ζ = 45°, there is early and significant anisotropy with the highest radial strain amplitude. The cases of ζ = 0°, 30°, 75° and 90° reach stability, while the cases of ζ= 15°, 60° and 45° still show rising values.

The cases of ζ = 75° and ζ = 90° show similar development curves with minimal anisotropy.

（2）Consistent torsional shear strain patterns occur across most ζ angles, with exceptions at ζ=90° and ζ=60°. Initial cycle fluctuations occur at ζ=90° and ζ=75°, while the cases of ζ=0° to ζ=60° follow a similar trend. The case of ζ=60° exhibits the highest initial fluctuation at 0.006%, stabilizing around 0.002%. Conversely, the cases of ζ=30° and ζ=45° show minimal anisotropy, closely coinciding in torsional shear strain during stress axis rotation.

（3）The consolidation angle has a notable impact on volumetric strain, indicating distinct anisotropic traits. When both factors are considered, during stress axis rotation, the initial rate of volumetric strain growth follows a linear trend. Yet, this growth rate gradually decreases over time, leading to a reduction in sample size.

（4）As the initial consolidation angle increases, the hysteresis curve shifts leftward, signifying cyclic creep behavior. At ζ=60°, there is a threshold for creep, with very small shear strain. With longer cycle periods, the hysteresis loop shrinks, and shear strain amplitude diminishes, indicating ongoing reinforcement and eventual stabilization of shear stiffness.

In addition, future research is needed to investigate the long term stress strain development behaviour and the effect of other parameters such as consolidation pressure and various intermediated consolidation coefficient.

Conflicts of Interest

The authors declared that they have no conflicts of interest to this work.

References

[1] SHAO W, CHEN Z, SHAO Y. Intergrading water quality parameters, benthic fauna and acute toxicity test for risk assessment on an urban-rural river[J]. Sustainability, 2023, 15(8): 6423.

[2] ZHUANG D, GUO W, SUN L. Effect of strain rate on triaxial extension behavior of silty clay[J]. Marine Georesources & Geotechnology, 2023, 41(4): 366−375.

[3] WANG W, CAO G, LI Y. Experimental study of dynamic characteristics of tailings with different reconsolidation degrees after liquefaction[J]. Frontiers in Earth Science, 2022, 10: 876401.

[4] LIU X Y, ZHANG X W, KONG L W. Effect of principal stress direction during consolidation on the shear strength properties of natural granite residual soil[J]. Soils and Foundations, 2022, 62(5): 101220.

[5] JEFFERIES M, SHUTTLE D, BEEN K. Principal stress rotation as cause of cyclic mobility[J]. Geotechnical Research, 2015, 2(2): 66−96.

[6] CAI Y, SONG X, SUN Q. Drained responses of granular soil sheared under inclined principal stress axes: impact of sample preparation[J]. Engineering Geology, 2018, 241: 33−40.

[7] WU T, CAI Y, GUO L. Influence of shear stress level on cyclic deformation behaviour of intact Wenzhou soft clay under traffic loading[J]. Engineering Geology, 2017, 228: 61−70.

[8] GUO L, CAI Y Q, JARDINE R J, et al. Undrained behaviour of intact soft clay under cyclic paths that match vehicle loading conditions[J]. Canadian Geotechnical Journal, 2018, 55(1): 90−106.

[9] SHI W J, WANG J, GUO L, et al. Undrained cyclic behavior of overconsolidated marine soft clay under a traffic-load-induced stress path[J]. Marine Georesources and Geotechnology, 2017, 36(1): 163−172.

[10] WANG J, FENG D, GUO L, et al. Anisotropic and noncoaxial behavior of K_0-consolidated soft clays under stress paths with principal stress rotation[J]. Journal of Geotechnical and Geoenvironmental Engineering, 2019, 145(9): 04019036.

[11] JARDINE R J, POTTS D M, FOURIE A B. Studies of the influence of non-linear stress–strain characteristics in soil–structure interaction[J]. Géotechnique, 1986, 36(3): 377−396.

[12] LI B, CHEN L L, GUTIERREZ M. Influence of the intermediate principal stress and principal stress direction on the mechanical behavior of cohesionless soils using the discrete element method[J]. Computers and Geotechnics, 2017, 86: 52−66.

[13] GEORGIANNOU V N, KONSTADINOU M, TRIANTAFYLLOS P. Sand behavior under stress states involving principal stress rotation[J]. Journal of Geotechnical and Geoenvironmental Engineering, 2018, 144(6): 04018028.

[14] QIAN J G, DU Z B, YIN Z Y. Cyclic degradation and non-coaxiality of soft clay subjected to pure rotation of principal stress directions[J]. Acta Geotechnica, 2018, 13(4): 943−959.

[15] WANG Y, GAO Y, GUO L. Influence of intermediate principal stress and principal stress direction on drained behavior of natural soft clay[J]. International Journal of Geomechanics, 2018, 18(1): 04017128.

[16] ZDRAVKOVIĆ L, JARDINE R J. The effect on anisotropy of rotating the principal stress axes during consolidation[J]. Géotechnique, 2001, 51(1): 69−83.

[17] SIVATHAYALAN S, VAID Y P. Influence of generalized initial state and principal stress rotation on the undrained response of sands[J]. Canadian Geotechnical Journal, 2002, 39(1): 63−76.

[18] HIGHT D W, GENS A, SYMES M J. The development of a new hollow cylinder apparatus for investigating the

effects of principal stress rotation in soils[J]. Géotechnique, 1983, 33(4): 355−383.

[19] MIURA K, MIURA S, TOKI S. Deformation behavior of anisotropic dense sand under principal stress axes rotation[J]. Soils and Foundations, 1986, 26(1): 36−52.

[20] KUMRUZZAMAN M, YIN J H. Influence of the intermediate principal stress on the stress–strain–strength behaviour of a completely decomposed granite soil[J]. Géotechnique, 2012, 62(3): 275−280.

[21] WANG Y, GAO Y, GUO L. Cyclic response of natural soft marine clay under principal stress rotation as induced by wave loads[J]. Ocean Engineering, 2017, 129: 191−202.

[22] SYMES M J P R, GENS A, HIGHT D W. Undrained anisotropy and principal stress rotation in saturated sand[J]. Géotechnique, 1984, 34(1): 11−27.

[23] SYMES M J, GENS A, HIGHT D W. Drained principal stress rotation in saturated sand[J]. Géotechnique, 1988, 38(1): 59−81.

[24] YOSHIMINE M, ISHIHARA K, VARGAS W. Effects of principal stress direction and intermediate principal stress on undrained shear behavior of sand[J]. Soils and Foundations, 1998, 38(3): 179−188.

[25] NAKATA Y, HYODO M, MURATA H. Flow deformation of sands subjected to principal stress rotation[J]. Soils and Foundations, 1998, 38(2): 115−128.

[26] YANG Z X, LI X S, YANG J. Undrained anisotropy and rotational shear in granular soil[J]. Géotechnique, 2007, 57(4): 371−384.

[27] ZHOU R, ZHANG F, ZHAO K. Experimental study on excess pore pressure and deformation of saturated silt under complex stress paths[J]. Journal of Natural Disasters, 2018, 27(6): 173−179.

[28] ZHANG F, CHEN G X, WU Q, et al. Experimental study on undrained behavior of saturated silt subject to wave loading[J]. Rock and Soil Mechanics, 2019, 40(7): 2695−2702.

[29] KANDASAMI R K, MURTHY T G. Experimental studies on the influence of intermediate principal stress and inclination on the mechanical behaviour of angular sands[J]. Granular Matter, 2015, 17(2): 217−230.

[30] KRISHANTHAN K. Influence of principal stress rotation on the behaviour of soft railway subgrade[D]. Wollongong: University of Wollongong, 2018.

[31] SAYAO A, VAID Y P. A critical assessment of stress nonuniformities in hollow cylinder test specimens[J]. Soils and Foundations, 1991, 31(1): 60−72.

[32] ZHUANG H, LI M, WANG C. The effects of initial deviatoric stress on anisotropy of marine clay and strain components[J]. Marine Georesources & Geotechnology, 2021, 39(10): 1167−1176.

[33] SKEMPTON A W. The pore-pressure coefficients *A* and *B*[J]. Géotechnique, 1954, 4(4): 143−147.

[34] TONG Z X, ZHANG J M, YU Y L. Drained deformation behavior of anisotropic sands during cyclic rotation of principal stress axes[J]. Journal of Geotechnical and Geoenvironmental Engineering, 2010, 136(11): 1509−1518.

[35] ZHOU J, YAN J J, XU C J. Influence of intermediate principal stress on undrained behavior of intact clay under pure principal stress rotation[J]. Mathematical Problems in Engineering, 2013, 2013: 950143.

[36] FAKHARIAN K, KAVIANI-HAMEDANI F, IMAM S M R. Influences of initial anisotropy and principal stress rotation on the undrained monotonic behavior of a loose silica sand[J]. Canadian Geotechnical Journal, 2022, 59(6): 847−862.

[37] LIAO D, YANG Z X. Hypoplastic modeling of anisotropic sand behavior accounting for rotation of principal stress direction[J]. Journal of Engineering Mechanics, 2022, 148(10): 04022060.

[38] WANG Y, GAO Y, LI B. Influence of initial state and intermediate principal stress on undrained behavior of soft clay during pure principal stress rotation[J]. Acta Geotechnica, 2019, 14(5): 1379−1401.

[39] QIAN Jian-gu, WANG Yong-gang, ZHANG Jia-feng, et al. Undrained cyclic torsional shear test on cumulative deformation of saturated soft clay under traffic dynamic loads[J]. Chinese Journal of Geotechnical Engineering, 2013, 35(10): 1790−1798.

[40] GUTIERREZ M, ISHIHARA K, TOWHATA I. Flow theory for sand during rotation of principal stress direction[J]. Soils and Foundations, 1991, 31(4): 121−132.

[41] YANG Y, YU H S. Application of a non-coaxial soil model in shallow foundations[J]. Geomechanics and Geoengineering, 2006, 1(2): 139−150.

[42] QIAN J G, YANG J, HUANG M S. Three-dimensional noncoaxial plasticity modeling of shear band formation in geomaterials[J]. Journal of Engineering Mechanics, 2008, 134(4): 322−329.

[43] WANG Y, GAO Y, CAI Y. Effect of initial state and intermediate principal stress on noncoaxiality of soft clay–involved cyclic principal stress rotation[J]. International Journal of Geomechanics, 2018, 18(7): 04018081.